applied sciences

MDPI

Article

The Effect of the Expression of the Antiapoptotic BHRF1 Gene on the Metabolic Behavior of a Hybridoma Cell Line

Iván Martínez-Monge [1,2,*], Pere Comas [2], David Catalán-Tatjer [1], Jordi Prat [2], Antoni Casablancas [2], Carlos Paredes [2], Martí Lecina [2,3] and Jordi Joan Cairó [2]

1 The Novo Nordisk Foundation Center for Biosustainability, Technical University of Denmark, DK-2800 Kongens Lyngby, Denmark; dacata@biosustain.dtu.dk
2 Chemical, Biological and Environmental Engineering Department, Campus Bellatera, Universitat Autònoma de Barcelona, Edifici Q, Carretera de Cerdanyola, s/n., 08193 Bellaterra, Spain; pere.comas@uab.cat (P.C.); jordipra60@yahoo.es (J.P.); antoni.casablancas@uab.cat (A.C.); carlesparedes@hotmail.com (C.P.); marti.lecina@iqs.url.edu (M.L.); JordiJoan.Cairo@uab.cat (J.J.C.)
3 Bioengineering Department, IQS-Universitat Ramon Llull, 08017 Barcelona, Spain
* Correspondence: ivanmar@biosustain.dtu.dk

Abstract: One of the most important limitations of mammalian cells-based bioprocesses, and particularly hybridoma cell lines, is the accelerated metabolism related to glucose and glutamine consumption. The high uptake rates of glucose and glutamine (i.e., the main sources of carbon, nitrogen and energy) lead to the production and accumulation of large amounts of lactate and ammonia in culture broth. Lactate and/or ammonia accumulation, together with the depletion of the main nutrients, are the major causes of apoptosis in hybridoma cell cultures. The KB26.5 hybridoma cell line, producing an IgG_3, was engineered with BHRF1 (KB26.5-BHRF1), an Epstein–Barr virus-encoded early protein homologous to the antiapoptotic protein Bcl-2, with the aim of protecting the hybridoma cell line from apoptosis. Surprisingly, besides achieving effective protection from apoptosis, the expression of BHRF1 modified the metabolism of the hybridoma cell line. Cell physiology and metabolism analyses of the original KB26.5 and KB26.5-BHRF1 revealed an increase of cell growth rate, a reduction of glucose and glutamine consumption, as well as a decrease in lactate secretion in KB26.5-BHRF1 cells. A flux balance analysis allowed us to quantify the intracellular fluxes of both cell lines. The main metabolic differences were identified in glucose consumption and, consequently, the production of lactate. The lactate production flux was reduced by 60%, since the need for NADH regeneration in the cytoplasm decreased due to a more than 50% reduction in glucose uptake. In general terms, the BHRF1 engineered cell line showed a more efficient metabolism, with an increase in biomass volumetric productivity under identical culture conditions.

Keywords: hybridoma; genome-scale metabolic model; antiapoptotic gene; mitochondrial transport; BHRF1

Citation: Martínez-Monge, I.; Comas, P.; Catalán-Tatjer, D.; Prat, J.; Casablancas, A.; Paredes, C.; Lecina, M.; Cairó, J.J. The Effect of the Expression of the Antiapoptotic BHRF1 Gene on the Metabolic Behavior of a Hybridoma Cell Line. *Appl. Sci.* **2021**, *11*, 6258. https://doi.org/10.3390/app11146258

Academic Editors: Alessandra Procentese and Francesca Raganati

Received: 14 June 2021
Accepted: 3 July 2021
Published: 6 July 2021

1. Introduction

The demand for monoclonal antibodies has significantly increased in recent years, mainly due to new applications in therapy, but also for clinical diagnoses and highly specific purification processes [1,2]. In this regard, the capacity of mammalian cells to perform complex post-translational modifications to yield biologically active proteins has led to their preferential use for biopharmaceuticals production. About 70–80% of all biopharmaceuticals, including monoclonal antibodies, viral vaccines and gene therapy vectors, are produced in mammalian cells. Among the top ten selling protein biopharmaceuticals in 2014, six were antibodies or antibody-derived proteins. It is therefore not surprising that in 2016, monoclonal antibody-based drug production using mammalian cell-based systems almost doubled that of 2010 [1,3]. In recent years, monoclonal antibodies indus-

trial manufacturing has been based on mammalian cell lines such as hybridoma, among others [3–6].

Mammalian cell-based processes present important limitations regarding apoptosis: the accumulation of metabolic byproducts (i.e., lactate and ammonia) up to cytotoxic concentration, and the depletion of essential nutrients, which triggers apoptosis (programmed cell death) [7]. The prevention of apoptosis during cell growth has a critical effect on the productivity of the final process, as an increase of cell life-span results in an increase in the synthesis and accumulation of the product of interest, since cells remain productive for a longer time, even after the exponential cell growth phase [8]. Moreover, more robust cell lines which are less sensitive to apoptosis make it possible to design high cell density culture strategies based on consistently low nutrient concentrations in narrower ranges [9].

In recent years, strategies to generate stress-resistant cell lines preventing apoptosis have been focused on blocking the apoptotic transduction pathways [10,11]. Although different pathways control the activation of signaling cascades of cell apoptosis activation, many of the apoptosis signals converge on the mitochondria, which stores numerous molecules that activate apoptosis [7]. The most widely used strategy to prevent apoptosis has been the overexpression of bcl-2 or bcl-xL genes, which inhibits the release of pro-apoptotic molecules from the mitochondria [10,12]. This strategy has been successfully applied in different mammalian cell lines, such as CHO or hybridoma, showing higher viabilities and improved robustness in cell culture [13–16]. The expression of mcl-1, another antiapoptotic gene with mechanism similar to that of bcl-2/bcl-xL, has also shown good results [17]. Another approach has been to directly target the caspase cascade, expressing X-linked inhibitor of apoptosis (XIAP) or cytokine response modifier CrmA, which both act to directly inhibit the caspases [18]. The expression of different viral proteins has also been reported to have antiapoptotic effects in hybridoma cell cultures, such as ksblc-2 from Karposi's sarcoma-associated herpesvirus [19] and bhrf-1 from Epstein-Barr virus [20]. Furthermore, the downregulation of the pro-apoptotic genes Bak, Bax and Casp3 has been shown to reduce apoptosis in CHO cells [21].

Additionally, antiapoptotic genes have been shown to have an effect on metabolism, although this is not yet fully understood [22,23]. This is remarkable, as cell-based processes present an important limitation regarding metabolism: deregulation of the uptake of substrates (i.e., high consumption rates of mainly glucose and glutamine), linked to the secretion and accumulation of lactate and ammonia as byproducts of metabolism [24].

The reduction of the secretion and accumulation of lactate remains a hot topic in the biomanufacturing industry. Many approaches have been explored to reduce or delay lactate generation in cell culture, including media design by the substitution of glucose for alternative sources of carbon, like fructose or galactose [25], different fed-batch strategies limiting glucose concentration [9,26] and several cell engineering approaches such as the expression of pyruvate carboxylase [27] and downregulation of lactate dehydrogenase [28]. In all of the described scenarios, a reduction, but never a total depletion, in lactate accumulation was observed.

In the present work, a murine hybridoma cell line (KB26.5) was engineered to overexpress the BHRF-1 gene (KB26.5-BHRF1). Besides the observed protective effect against apoptosis, the overexpression of BHRF-1 had an unexpected direct effect on cell physiology and metabolism. Mainly higher cell growth rate and more efficient nutrient usage were observed in batch cultures, significantly reducing the production of lactate. Therefore, metabolic flux balancing techniques were applied to better understand the interactions and effects of BHRF-1 expression with cell metabolism. Analysis of the obtained intracellular fluxes provided us with a better understanding of the effects of BHRF-1 expression on the improved cell metabolism, and gave rise to some hypotheses about possible BHRF-1 interactions with the metabolic pathways. Nowadays, the prevention of apoptosis continues to be a relevant research topic, e.g., in a review by Henry et al. (2020) [11], the effects of the various antiapoptotic strategies which have been applied in recent years were presented and discussed.

2. Materials and Methods

2.1. Cell Lines and Cell Maintenance

The murine hybridoma cell line used in this work was KB26.5, which produced an IgG_3 antibody against antigen A1 of human red blood cells (used to distinguish among ABO groups in blood tests). The KB26.5 cell line was transfected with BHRF1 (BamHI rightward reading frame 1)-enconding vector, as described by Juanola et al. (2009) [20].

Both cells lines were maintained in a 125 mL polycarbonate shake flask (Corning Inc., Corning, NY, USA) with a working volume of 20 mL, incubated in a humidified atmosphere at 37 °C with 5% CO_2 (Steri-cult 2000 Incubator). The agitation was set at 110 rpm with an orbital shaking platform (Stuart SSL110). Cell passaging was performed every 2 or 3 days at an initial seeding density of $1.5 \cdot 10^5$ cells/mL.

2.2. Culture Medium

Dulbecco's modified Eagle's media (DMEN) (D5796, Sigma, St. Louis, MO, USA), containing 25 mM glucose and 4 mM glutamine, was used. Basal media was supplemented with 2 mM glutamine (Sigma), 5% FBS (*v/v*) (Sigma), 0.5% Antifoam C Emulsion (Sigma) and 2% Kolliphor® P 188 (Sigma).

2.3. Shake-Flasks Culturing Platform

A set of 250 mL polycarbonate shake-flask (Corning Inc.) with 50 mL working volume was used for preliminary experiments. Identical conditions to those described under "cell maintenance" were maintained. The seeding density was about 3.0×10^5 cells/mL, and the sampling volume was 1 mL.

2.4. Bioreactor and Operational Conditions

Bioreactor cell cultures were run in a 2 L Biostat Bplus (Sartorius Stedim Biotech, Gottingen, Germany). The bioreactor was equipped with the necessary probes to maintain the desired culture conditions regarding pH, pO_2 and temperature, stirred with two marine impellers at 60 rpm. The dissolved oxygen (DO) concentration was measured with an optical probe (VisiFerm DO, Hamilton). DO was set at 40% saturation with a constant aeration inflow of 0.20 L/min, with variable composition controlled by a gas mix air/oxygen station. pH was measured with a standard electrode (EASYFERM PLUS, Hamilton) and maintained at 7.1 through the addition of NaOH 0.5 M solution when buffer capacity was not enough to compensate for acidification. CO_2 inlet gas enrichment was fixed at 5% during the entire process. The temperature was set at 37 °C.

2.5. Analytical Methods

2.5.1. Cell Number

Cell number was determined by manual counting using a Neubauer hemocytometer and a phase contrast microscope (Nikon eclypse TS100). Cell viability was determined by the trypan blue dye exclusion method (1:1 mixture of a 0.2% trypan blue (Gibco Thermo Fisher Scientific, Waltham, MA, USA) in phosphate buffer saline and cell sample).

2.5.2. Metabolite Concentrations

For the metabolite analysis, samples were centrifuged at $3000\times$ *g* for 3 min (Spectrafuge) and the pellet was discarded. Daily measurements of centrifuged samples were taken for glucose, lactate, glutamine, glutamate, ammonia, K^+, Na^+ and osmolality, using the BioProfile 400 (Nova Biomedical, Waltham, MA, USA).

Prior to the amino acid analysis, supernatants were filtrated using 96-well filter plates (AcroPrep Advance, 0.2 µm Supor Short Tip Natural PP, Pall Corporation, New York, NY, USA). Amino acids were quantified using a method based on that of Valgepea et al. (2017) with the following modifications: amino acids were derivatized in the HPLC autosampler (Dionex Ultimate 3000), and the sample was injected into an AdvanceBio AAA (2.7 um, 4.6 × 100 mm, Agilent PN: 655950-802) with a guard column (AdvanceBio AAA 2.7 um,

4.6 × 5 mM PN: 820750-931). The HPLC gradient was 5–22% B from 0–7 min, 22–23% B from 7–8 min, 23–30% B from 8–9 min, 30–40% B from 9–14 min, 40–50% B from 14–16 min, 50–55% B from 16–18 min, 55–100% B from 18–18.5 min and kept at 100% to 20.1 min, but decreased to 5% B until 24 min, when chromatography was completed. Buffer A was 40 mM Na_2HPO_4, 0.02% NaN_3 (*w/v*) at pH 7.8. Buffer B was 45% (*v/v*) acetonitrile, 45% (*v/v*) methanol and 10% (*v/v*) water. Flow rate was 1 mL/min from 0–18.5 min, 1.5 mL/min from 18.5–22.1 min, and thereafter, 1 mL/min to 24 min. Derivatized amino acids were monitored using a fluorescence detector. OPA-derivatized amino acids were detected at 340ex and 450em nm, and FMOC-derivatized amino acids at 266ex and 305em nm. Quantifications were based on standard curves derived from serial dilutions of an in-house prepared mixed amino acid standard. The upper and lower limits of quantification were 75 and 0.5 µg/mL, respectively. Chromatograms were integrated using Chromeleon version 7.1.3.

2.5.3. Product Concentration

Product concentration was measured using Valita® TITER Assay at the moment the cells reached the maximum density in bioreactor. The Valita® TITER Assay is a fluorescence polarization assay for the quantitative detection of IgG antibodies in cell culture. Standard curve was performed using a known concentration IgG standard (Human IgG Isotype Control, Thermo Fisher, Waltham, MA, USA) diluted in the same cell culture media as that used in the experiments. An eight-point standard curve performed in triplicated was used. The Valitacell Evaluation tool software was used to analyze the titer assays.

2.6. Oxygen Uptake Rate (OUR)

Determination of the oxygen uptake rate (OUR) was performed by applying the dynamic method [29,30]. This method is based on interrupting the air inflow to the bioreactor for a few minutes; then, the dissolved oxygen concentration decreases due to the respiratory activity of the cells and to the oxygen desorption from the liquid phase to the bioreactor headspace. The specific methodology used in this work is detailed in the literature [31,32].

2.7. Estimation of Specific Consumption and Production Rates

The methodology followed to calculate the specific consumption and production rates for the metabolites analyzes is detailed in a report by Martínez-Monge et al. (2019) [33].

The specific productivity (q_p) of the cells in the process was calculated using the integral of viable cells (IVC) and the product concentration between the first and last points, as presented in Equation (1). IVC was calculated using the trapezoidal rule with the function trapz included in MATLAB 2019a (Mathworks).

$$q_p = \frac{[\text{Product}]_{\text{final}}}{\text{IVC}} \quad (1)$$

For volumetric productivity (V_P), the final product concentration and the total process time was used, as shown in Equation (2).

$$V_P = \frac{[\text{Product}]_{\text{final}}}{t_{\text{total}}} \quad (2)$$

2.8. Reduced Genome-Scale Metabolic Model

In this study, the reduced genome scale metabolic model published by Martínez et al. (2013) [34] was further modified to adapt it to the experimental conditions. The original model is freely available in Systems Biology Markup Language (SBML) [34]. The model was derived from the complete Hybridoma genome-scale metabolic model constructed from a generic genome-scale metabolic model of *Mus musculus* [35,36]. The adaptation process to obtain a reduced model which is able to perform flux analysis for the experiments performed in hybridoma was detailed in Martínez-Monge et al. (2019) [33]. The base

metabolic model did not contain the biomass formation equation, since the defined objective function depended on maximizing or minimizing of the ATP yield. So, the base model was modified by adding 14 reactions involved in the synthesis of all of the metabolite precursors needed for biomass formation, as detailed in Martínez-Monge et al. (2019) [33]. The final model is composed of 362 internal and 36 external reactions that collectively involve 395 metabolites. A complete list of all included reactions and metabolites is available in the Supplementary Data 1 in xlsx format.

2.9. Flux Balance Analysis of the Reduced Model

A Parsimonious Flux Balance Analysis (p-FBA) was performed using Optflux 3.4 Software [37], a user-friendly computational tool for metabolic engineering applications. p-FBA is a variant of flux balance analysis that minimizes the total material flow to achieve an objective while maintaining optimal growth [38]. A graphical representation of the p-FBA was generated using the Omix Visualization Software (GmbH&Co.KG), as described by Droste et al. (2011) [39], in which only the most significant fluxes for this study were represented.

As usual in FBA with genomic models, the system was underdetermined with some degrees of freedom. To find the optimal state, p-FBA optimizes a certain objective function, in this case, the maximum value of ATP generation (EF0002). The cytoplasmic malic enzyme was considered to be inactive, and NADPH required for biosynthesis could only be regenerated by the pentose phosphate pathway, as this degree of freedom can only be resolved by using more advanced fluxomic techniques (R00216 [0 0]) [40]. Glutaminolysis was constrained to go in the direction of oxoglutarate generation (R00243mitoc [0 10000]) [41]. The specific consumption/production rates of the measured experimental metabolites were added to the model using the mean of the duplicates ± standard deviation.

3. Results

3.1. Effect of BHRF1 on Cell Physiology

3.1.1. Noncontrolled Culture Conditions: Shake Flask Cultures

After engineering KB26.5 hybridoma cell lines with the BHRF1 gene, the transformed cell population was kept under selective pressure for several passages. Then, differences in cell physiology between the cell line KB26.5 and the engineered KB26.5-BHRF1 were observed after comparing both cell lines in shake flask cultures. The time profiles for cell growth, cell viability, glucose and lactate concentrations for both cell lines (A1 for KB26.5 and B1 for KB26.5-BHRF1) are displayed in Figure 1. A Napierian logarithm of viable cells versus time is plotted to better understand the variations in cell growth, as will be discussed later (A2 for KB26.5 and B2 for KB26.5-BHRF1). Considering that the experiments were carried out in duplicate (same time points), the mean values are plotted together with the standard deviation.

The parental KB26.5 cell line reached a cell density of $1.79 \pm 0.3 \times 10^6$ cells/mL after 72 h of culture, at which point cell viability decreased sharply. In contrast, KB26.5-BHRF1 reached $3.92 \pm 0.03 \times 10^6$ cell/mL in about the same time. Regarding glucose and lactate concentration, high consumption and production rates respectively could be deduced by the sharp decay/increase of the concentration profiles, obtaining more lactate generation in the parental KB26.5 cell line. The slopes of the Napierian logarithm plots of viable cells showed a higher cell growth rate for the KB26.5-BHRF1 compared with the parental line. Parallel to the plateau of the cell growth profile, glucose consumption and lactate production also indicated a metabolic arrest at 72 h of culture, when their concentration values became almost constant. No morphology changes were observed between KB26.5 and KB26.5-BHRF1 on different days from manual counting using a microscope (data not shown).

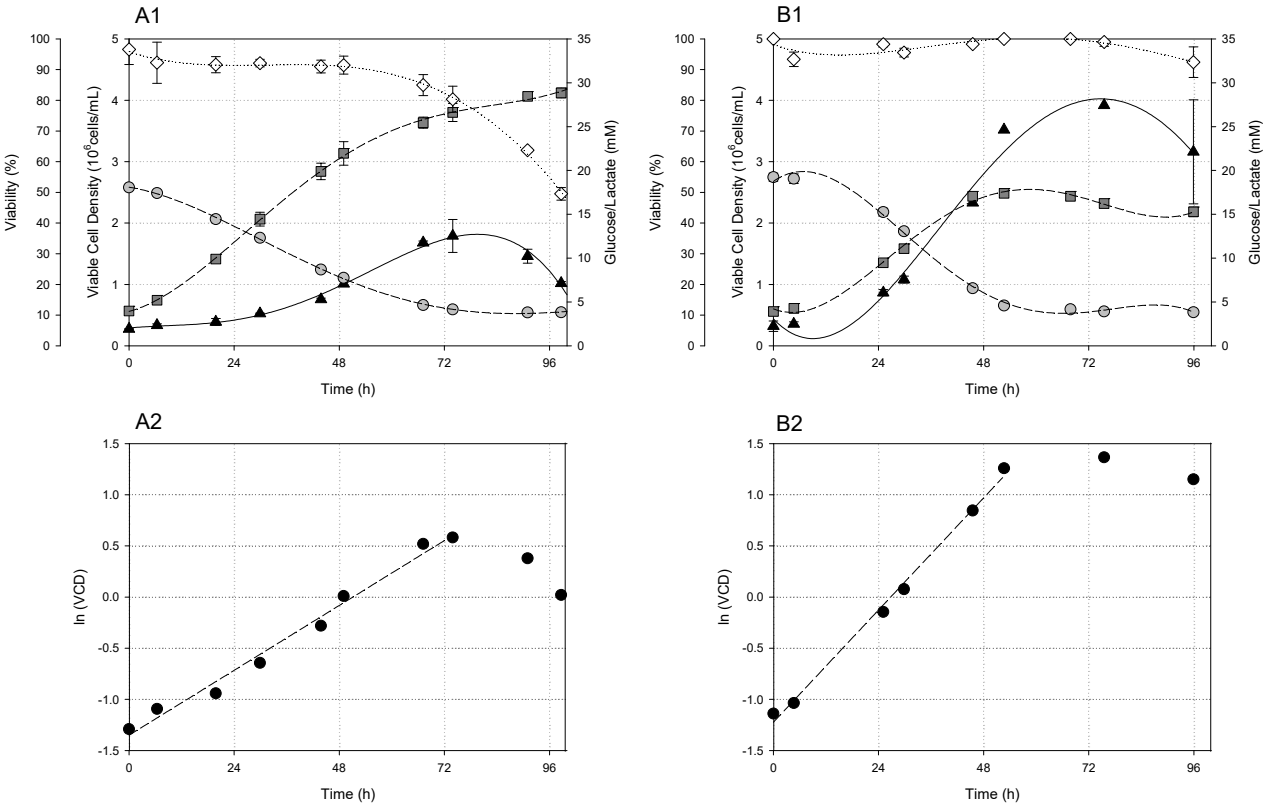

Figure 1. Time profile of viable cell density (▲), cell viability (◊), glucose (●) and lactate (■) concentration of batch cultures run in shake flasks ((**A1**): parental KB26.5 and (**B1**): engineered KB26.5-BHRF1). Napierian logarithm of viable cell density versus time (•) ((**A2**): parental KB26.5 and (**B2**): engineered KB26.5-BHRF1). Data obtained from duplicate cultures in shake flasks; the error bar corresponds to the standard deviation.

3.1.2. Controlled Bioreactor Cultures

In order to confirm the beneficial effect of BHRF1 on cell physiology (i.e., on cell growth and nutrients usage), cultures of both cell lines were performed in a 2 L bioreactor. Bioreactor cultures should not only allow us to disregard the possibility that the differences encountered previously were related to the changing conditions when culturing cells in shake flasks (non pH and dissolved oxygen control), but also to generate enough data to perform the flux balance analysis. In addition, product concentration (IgG_3) was measured from the moment the cells reached the maximum density. Figure 2 shows the time profile of cell density and viability, as well as the evolution of glucose, lactate and product concentrations. As the experiments were carried out in the same bioreactor in duplicate but not in parallel (different time points), both replicates are plotted for each cell line, showing comparable behavior. A Napierian logarithm of viable cells versus time is plotted for each replicate in Figure 3, to better understand the changes in cell growth. The results show the same behavior encountered in the previous shake-flask experiments, i.e., KB26.5-BHRF1 showed higher final cell density, higher growth rate and less lactate production. The final titer obtained was also higher for KB26.5-BHRF1.

Finally, before preforming flux balance analysis (FBA), the specific consumption rates for all the metabolites measured in bioreactor experiments were calculated in the exponential growth phase (Table 1). Values were calculated as the mean of the data obtained from duplicate cultures. In general, KB26.5-BHRF1 showed more efficient substrate consumption (especially for glucose and glutamine), and reduced byproduct generation (especially lactate, ammonia and alanine).

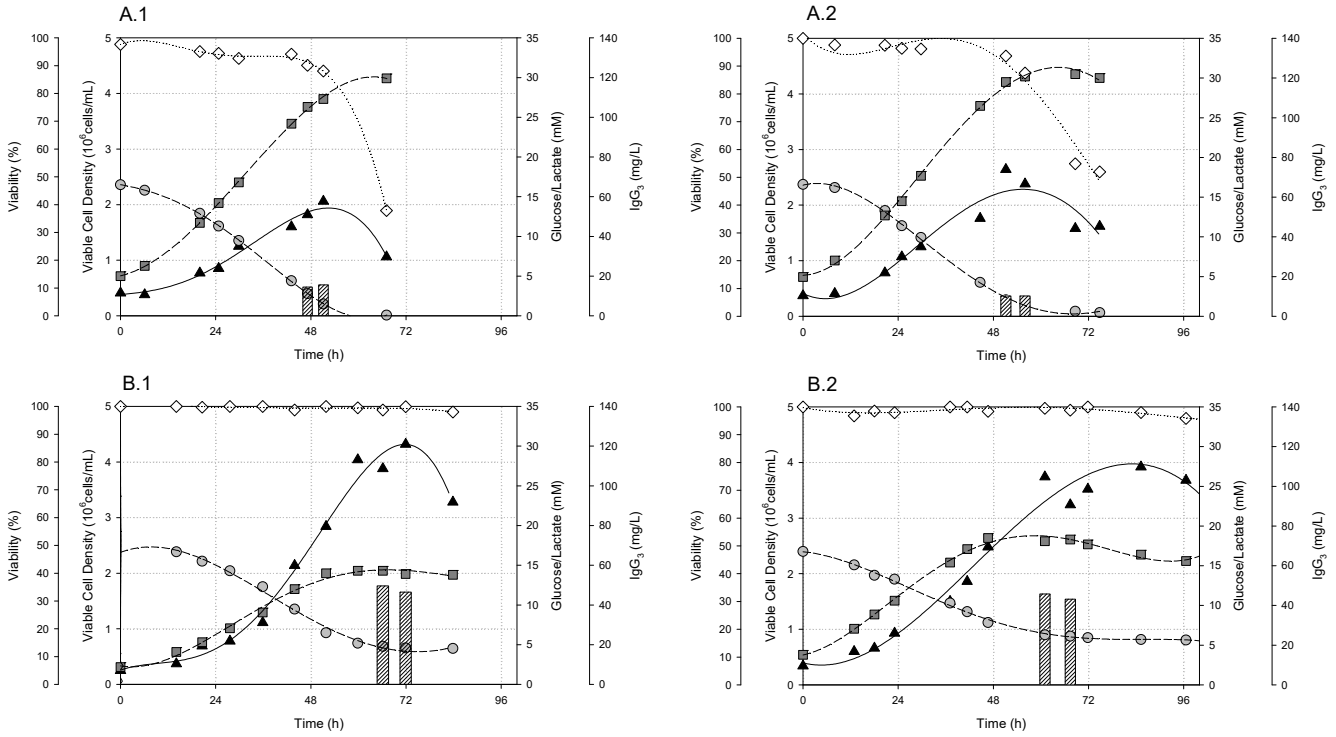

Figure 2. Two L bioreactor batch cultures of the parental KB26.5 cell line (**A.1** and **A.2**) and the engineered KB26.5-BHRF1 (**B.1** and **B.2**). Time profile of cell density (▲), cell viability (◊); glucose (●) and lactate (■) and product (bars) concentration of batch cultures. Duplicate cultures are shown for each cell line.

3.2. Effect of BHRF1 on Cell Metabolism: Flux Balance Analysis

The metabolism of animal cells growing in high glucose media is characterized by high rates of glycolysis fluxes. The metabolism of glucose by aerobic microorganisms yields pyruvate, which is partially converted into acetyl-CoA, and then completely oxidized to CO_2 and H_2O in the TCA cycle. However, in mammalian cell lines, pyruvate is primarily converted into lactate [24]. The generation and accumulation of large amounts of lactate, since glucose cannot be completely oxidized, is the major consequence of such high glycolytic fluxes, leading to unbalanced metabolism. This metabolic behavior has been observed in hybridoma cell lines, regardless of the level of dissolved oxygen in the culture. Lactate generation from pyruvate seems to be necessary to fulfill the NADH regeneration requirements in the cytoplasm [42] due to the limiting transport rates of NADH into the mitochondria, where it can also be regenerated, even though lactate formation is a much less energetically efficient process than its oxidation in the Krebs cycle [34].

Flux Balance Analysis (FBA) is a useful tool to obtain information about the redistribution of internal metabolic fluxes. It also helped us to generate some hypotheses about the effects of BHRF1 on metabolism. Figures 4 and 5 show the distribution of the metabolic fluxes using the genome-derived model for *Mus musculus*. Metabolic flux balances were conducted using the data obtained from the bioreactor cultures.

FBA led to deregulated metabolism in both cell lines, characterized by high glycolytic fluxes and consequent lactate generation and secretion. However, glycolytic fluxes were reduced by 54% (bottom part of glycolysis as a reference) due to the reduction in glucose consumption (51%) in KB26.5-BHRF1. Lactate generation flux dropped more than 60%. Despite the lower fluxes in glycolysis presented by the KB26.5-BHRF1 strain compared to KB26.5, the rate of carbon influx from cytoplasm to mitochondria through pyruvate was 14% higher (320 versus 274 nmol/(mg·h)). In other words, when calculating the fluxes in mass units (mg metabolite/(mg DCW·h)), only 13% of the total glucose consumed had entered the mitochondria of KB26.5 cells, whereas this increased to 32% in the engineered

KB26.5-BHRF1. When performing similar calculations to estimate the lactate generation ratio regardless of glucose consumption, lactate formation represented about 87% and 69% of the consumed glucose in KB26.5 and KB26.5-BHRF1 respectively.

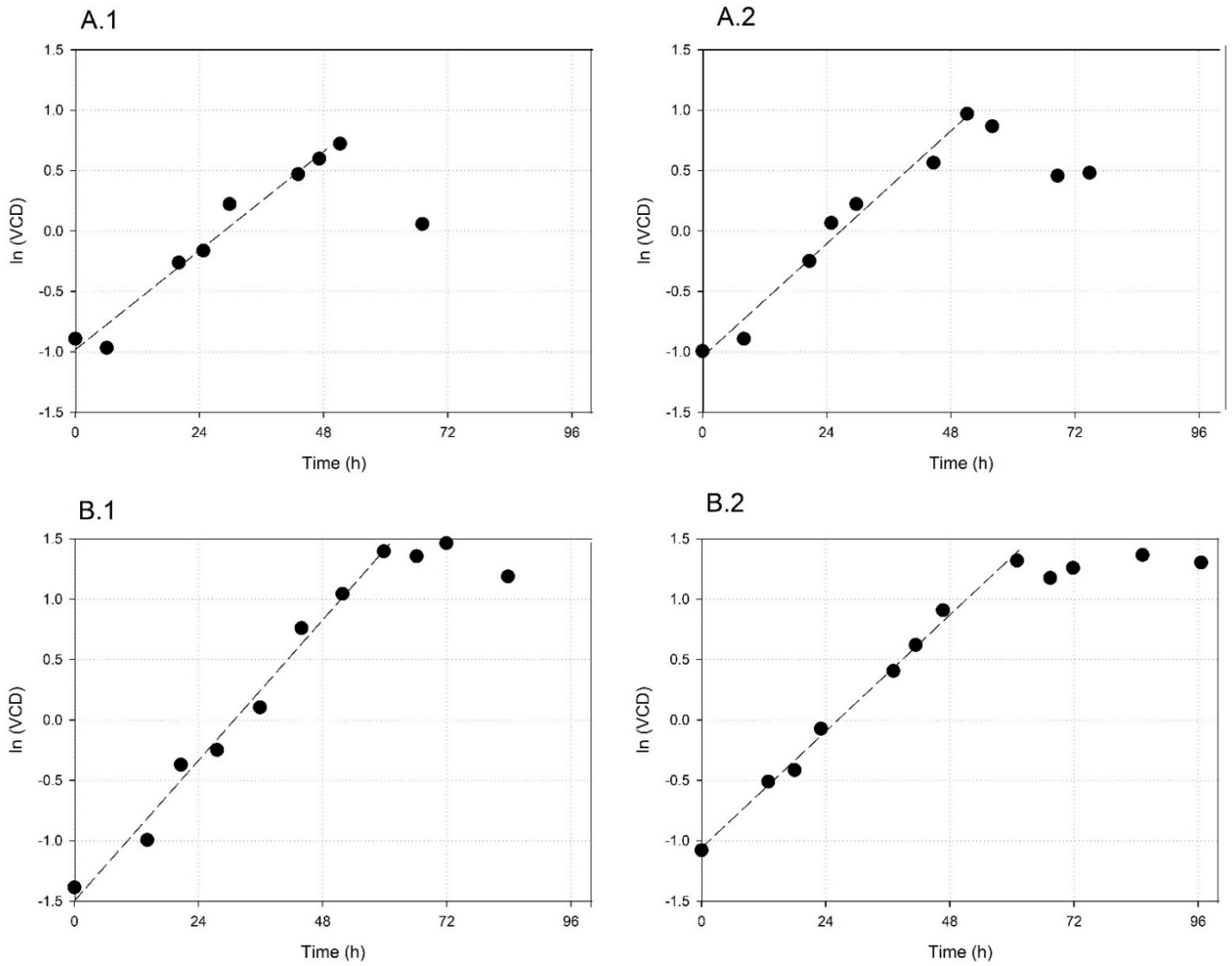

Figure 3. Two L bioreactor batch cultures of the parental KB26.5 cell line (**A.1** and **A.2**) and the engineered KB26.5-BHRF1 (**B.1** and **B.2**). Napierian logarithm of viable cell density versus time (•). Duplicate cultures are presented for each cell line.

Table 1. Specific consumption rates of glucose, amino acids and oxygen, and production rates of lactate and ammonia for KB26.5 and KB26.5-BHRF1 cell lines. Cultures were run in 2 L bioreactors. The specific rates are part of the 38 external measured fluxes used as modeling constraints, and are expressed in nmol/(mg·h) units.

Parameter (nmol/mg·h^{-1})	KB26.5	KB26.5-BHRF1
Alanine	132.493 ± 12.954	48.305 ± 4.158
Arginine	−14.726 ± 2.812	−15.517 ± 8.825
Asparagine	5.420 ± 1.302	3.058 ± 0.681
Aspartic acid	4.304 ± 6.017	0.487 ± 0.801
Biomass	0.036 ± 0.006	0.048 ± 0.007
Cysteine	−5.024 ± 2.111	−4.825 ± 4.079
Glucose	−933.447 ± 134.567	−542.206 ± 177.457
Glutamic acid	7.858 ± 0.265	0.841 ± 0.956
Glutamine	−258.541 ± 76.627	−179.660 ± 122.421
Glycine	−11.597 ± 6.102	−12.094 ± 6.784

Table 1. *Cont.*

Parameter (nmol/mg·h^{-1})	KB26.5	KB26.5-BHRF1
Histidine	−6.744 ± 3.693	−5.368 ± 3.796
Isoleucine	−24.989 ± 5.918	−18.098 ± 16.359
Lactate	1435.500 ± 348.745	654.556 ± 34.663
Leucine	−28.854 ± 6.149	−24.593 ± 17.043
Lysine	−22.759 ± 9.314	−21.579 ± 17.480
Methionine	−7.315 ± 0.948	−6.511 ± 4.841
$NH4^+$	156.137 ± 11.064	85.090 ± 15.910
Phenylalanine	−9.685 ± 2.050	−10.009 ± 8.848
Proline	13.080 ± 4.084	1.993 ± 8.586
Oxygen	−701.500 ± 160.513	−674.500 ± 12.021
Serine	−15.150 ± 6.181	−13.913 ± 11.826
Threonine	−16.883 ± 3.216	−18.522 ± 18.500
Tryptophan	−2.585 ± 3.297	−1.078 ± 0.722
Tyrosine	−8.340 ± 1.832	−8.392 ± 7.974
Valine	−24.539 ± 4.938	−20.236 ± 18.013

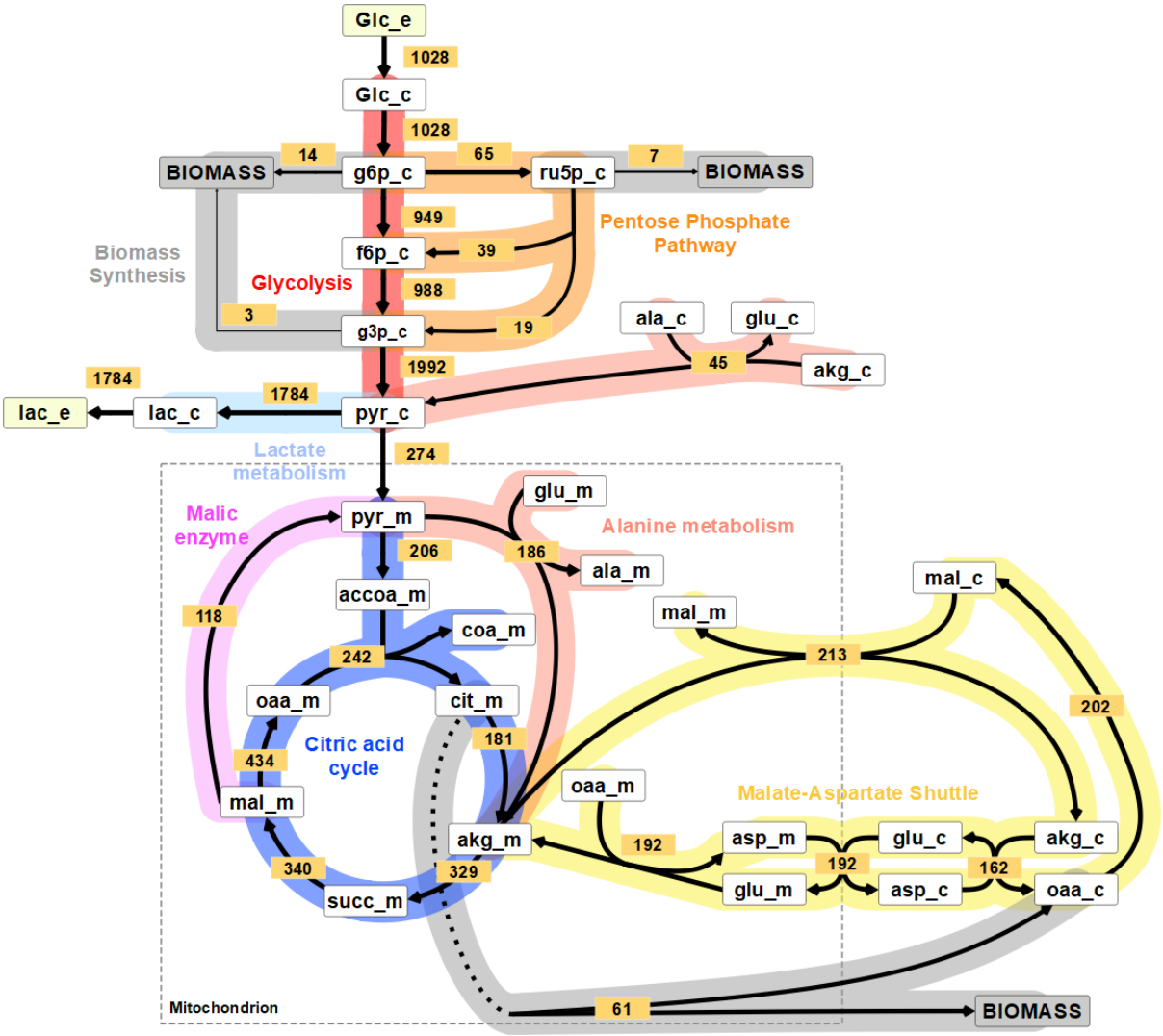

Figure 4. Metabolic flux distribution of the parental KB26.5 hybridoma cell line. The arrows indicate the direction of the reaction; the arrow thickness is proportional to the flux rate. Different coloring was used for each pathway, and the model was structured in cytoplasmic and mitochondrial reactions (mitochondrion is limited by a discontinued line). The values in the boxes correspond to the flux rate in nmol metabolite/(mg DCW·h).

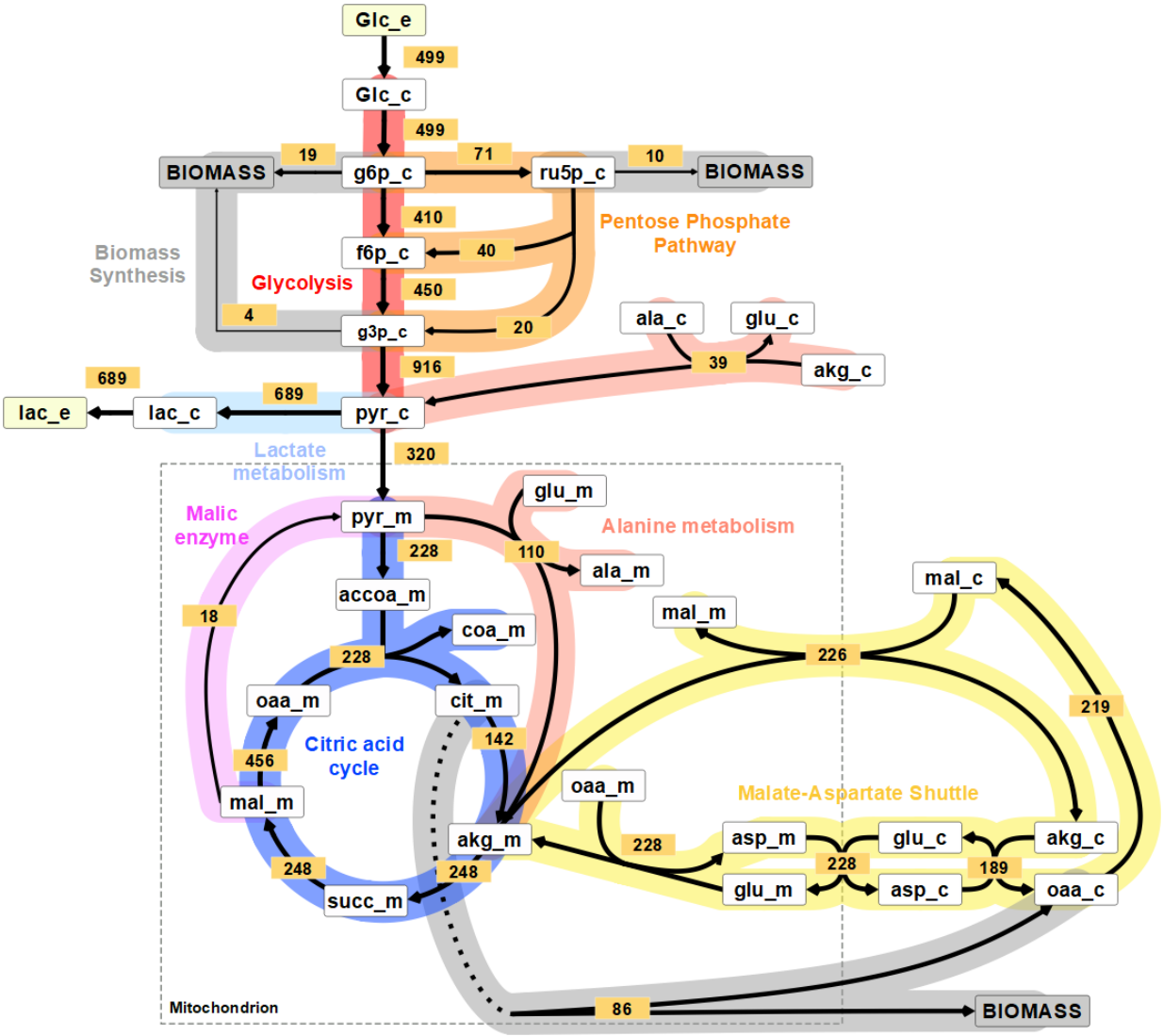

Figure 5. Metabolic flux distribution of the engineered hybridoma cell line KB26.5-BHRF1. The arrows indicate the direction of the reaction; the arrow thickness is proportional to the flux rate. Different coloring was used for each pathway, and the model was structured in cytoplasmic and mitochondrial reactions (mitochondrion is limited by a discontinued line). The values in the boxes correspond to the flux rate in nmol metabolite/mg DCW·h.

In this case, FBA shows that the rate of transport of reduction power from cytoplasm to mitochondria through the malate-aspartate shuttle seems to be a bit higher in KB26.5-BHRF1 than in KB26.5, with a 19% increase, i.e., a rate of 228 versus 192 nmol/(mg·h) in the aspartate-glutamate mitochondrial symport transport. However, in both cases, the high glycolytic fluxes caused the cells to generate lactate, as the malate-aspartate shuttle seemed to be insufficient to couple with the cytoplasmic NADH regeneration. In addition, a slight increase in the pathways related with the formation of a biomass was observed in KB26.5-BHRF1 due to the higher growth rate; as Pentose Phosphate Pathway to generate nucleotides or citrate export from the mitochondria to generate lipids.

Due to the high growth rate of KB26.5-BHRF1, an increase in the TCA fluxes was to be expected, producing more energy and, therefore, increased biomass. However, in comparing the TCA cycles for both cell lines, no significant increase was observed, which was in accordance with the similar observed oxygen consumption rate (Table 1). What is clear from the FBA is that there was a collapse between glycolysis and the TCA pathways in both cases, as the high glucose uptake rate collapses the transport of NADH to

mitochondria, and NADH have to be regenerated in cytoplasm using pyruvate by means of lactate dehydrogenase.

The reduction of the glycolytic pathway in KB26.5-BHRF1 involved a reduction of ATP production in the cytoplasm, as well as a reduction of NADH formation. Consequently, the need to oxidize the NADH formed in the cytoplasm also decreased, and, together with the slightly higher rates related to Malate-Aspartate Shuttle, yielded to a reduction in the formation of lactate. To further examine the results, an analysis of the synthesis and consumption of ATP was performed. Figure 6 shows the distribution of ATP formation (with regard to the reaction in which ATP was generated) and its consumption.

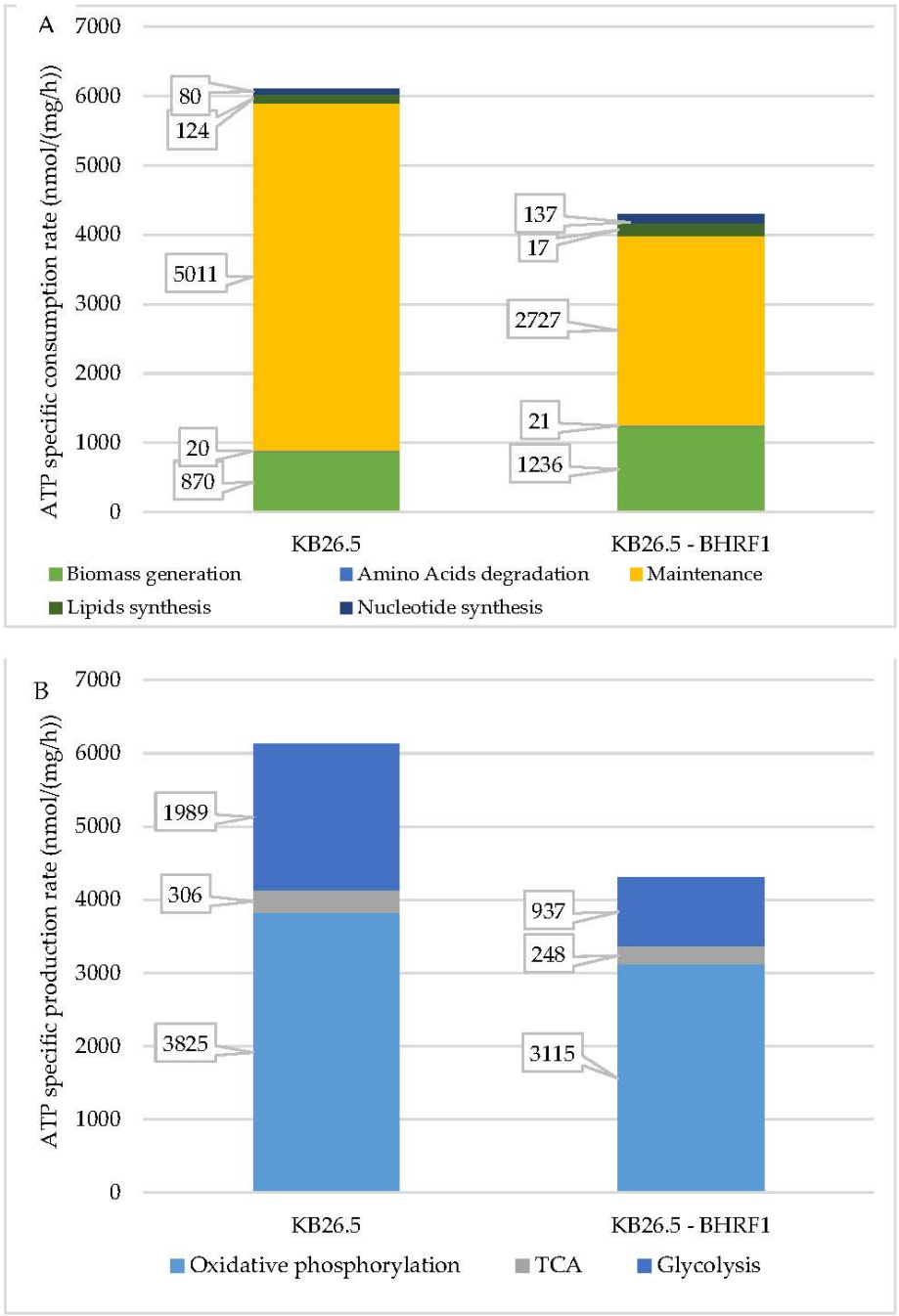

Figure 6. Distribution of ATP generation (concerning the reaction in which ATP was generated) and consumption in the KB26.5 and KB26.5-BHRF1 cell lines. ATP generation (**A**) and consumption (**B**) (nmol ATP/ (mg DCW·h)).

The results show a significant reduction in the total ATP generation and, as a consequence, ATP consumption in KB26.5-BHRF1, compared with the parental cell line. As pointed out above, higher amounts of ATP were synthetized during glycolysis in parental KB26.5 (in proportion with the increase in glycolytic flux). However, an increase in the oxidative phosphorylation pathway was also observed; this is very important for the present discussion, given its high capacity to generate ATP. Regarding ATP consumption, KB26.5-BHRF1 needs more ATP to generate more biomass, which also includes other pathways such as lipids and nucleotides generation.

4. Discussion

The growth, viability, glucose and lactate profiles obtained from the KB26.5-BHRF1 cultures were vastly different than those from the parental cell line. Cell culture expansion was much faster, and the maximum cell density reached $3.92 \pm 0.03 \times 10^6$ cell/mL, representing a two-fold increase. Additionally, the cell viability profile after the cell density peak remained at over 90% for 24 h after the maximum cell density had been achieved, indicating a delay in apoptosis due to the effects of BHRF1, as anticipated by Juanola et al. (2009) [20]. The glucose and lactate profiles showed an initial phase of glucose consumption and lactate generation. The glucose concentration profile decrease was similar to that obtained in the KB26.5 culture, but lactate production rates were reduced by almost half. However, since the cell density almost doubled, the specific glucose consumption rate was affected by BHRF1 expression and, consequently, by lactate production. In order to better quantify the differences, Table 2 presents the main physiological parameters for both cell lines, i.e., growth rate (μ), doubling time (t_d), specific glucose consumption rate (q_{Glu}), specific lactate production rate (q_{Lac}), glucose yield on biomass ($Y_{Glu/X}$), lactate yield on biomass ($Y_{Lac/X}$) and maximum VCD (VCD_{max}).

Table 2. Main physiological parameters determined for KB26.5 and KB26.5-BHRF1 in shake flask cultures. Values were calculated as the means of data obtained from duplicate cultures.

Parameter	KB26.5	KB26.5-BHRF1
μ (h^{-1})	0.027 ± 0.001	0.048 ± 0.002
t_d (h)	25.500 ± 0.928	14.560 ± 0.627
q_{Glu} (nmol/(mg·h))	-802.325 ± 71.750	-682.100 ± 55.536
q_{Lac} (nmol/(mg·h))	1337.750 ± 175.857	663.780 ± 13.831
$Y_{Glu/X}$ (mmol/L)/(10^6 cell/mL)	14.515 ± 0.120	4.645 ± 0.007
$Y_{Lac/X}$ (mmol/L)/(10^6 cell/mL)	24.265 ± 1.039	5.035 ± 1.704
VCD_{max} (10^6 cell/mL)	1.79 ± 0.30	3.92 ± 0.03

In general terms, the expression of BHRF1 was beneficial for cell physiology and growth. The cell growth rate (μ) increased by 78%, the specific glucose consumption rate (q_{Glu}) decreased by 15% and the specific lactate production rate (q_{Lac}) reduced by more than 50%. This resulted in a decrease in both glucose yield on biomass ($Y_{Glu/X}$) and lactate yield on biomass ($Y_{Lac/X}$) in KB26.5-BHRF1, meaning that more efficient glucose consumption had been achieved, thereby generating less lactate. Overall, this resulted in a more efficient use of the main carbon source. This fact translated into a more than two-fold increase in total cell density under the same media and culture conditions.

The results obtained in 2 L bioreactors showed similarities to those observed in shake flask cultures. The maximum cell density was slightly improved for KB26.5, reaching $2.34 \pm 0.39 \times 10^6$ cell/mL, probably due to the pH control. Even though lactate was produced at similar rates, the lack of pH control in the shake flaks might have negatively affected cell growth, a phenomenon which was reversed in the bioreactor cultures. In the case of KB26.5-BHRF1, the maximum cell density observed was significantly increased, reaching $3.93 \pm 0.01 \times 10^6$ cell/mL. In addition, the viability strongly decayed after 48 h for KB26.5, while it was maintained at above 90% in BHRF1-KB26.5.

Despite the concordance with the results observed in the shake flask cultures, another difference was that the glucose was completely depleted in the KB26.5 culture, indicating the extension of the culture time due to the pH control, which may have had an effect on cell density increase. To further compare the performance of both strains in the bioreactor, the main physiological parameters were calculated and compiled in Table 3, including maximum titer obtained (IgG_3,max), specific productivity (q_P) and volumetric productivity (V_P).

Table 3. Main physiological parameters determined for KB26.5 and KB26.5-BHRF1 cultures in 2 L bioreactors. Values were calculated as the means of data obtained from duplicate cultures.

Parameter	KB26.5	KB26.5-BHRF1
μ (h^{-1})	0.036 ± 0.006	0.048 ± 0.007
t_d (h)	19.823 ± 3.588	14.593 ± 2.001
q_{Glu} (nmol/(mg·h))	−933.447 ± 134.567	−542.206 ± 177.457
q_{Lac} (nmol/(mg·h))	1435.500 ± 348.745	654.556 ± 34.663
$Y_{Glu/X}$ (mmol/L)/(10^6 cell/mL)	8.805 ± 0.361	3.735 ± 0.346
$Y_{Lac/X}$ (mmol/L)/(10^6 cell/mL)	14.010 ± 0.665	4.730 ± 1.160
VCD_{max} (10^6 cell/mL)	2.34 ± 0.39	3.93 ± 0.01
IgG_3,max (mg/L)	12.90 ± 3.82	47.70 ± 2.69
q_P (µg/(10^6 cell·h))	0.24 ± 0.08	0.48 ± 0.02
V_P ((µg/L)/h)	252.12 ± 74.63	750.22 ± 0.85

Similar to shake flask culture results, cell growth improved by more than 30% in KB26.5-BHRF1, with a reduction of 42% and 54% in specific glucose consumption rate and specific lactate production rate, respectively. Therefore, the differences between strains may have been related to the effects of BHRF1 on cell physiology, rather than a consequence of the culture conditions. The same was observed regarding glucose and lactate yield on biomass, as both were reduced in KB26.5-BHRF1. Due to the extension of the growth phase, KB26.5-BHRF1 increased the final product concentration by 3.7 times. The specific and volumetric productivity were also increased two- and three-fold, respectively.

The results showed lower specific consumption rates for glucose and almost all amino acids, as well as lower production rates of byproducts, which might indicate efficient cell metabolism mediated by the expression of BHRF1. Additionally, the significant reduction in glutamine consumption, and therefore, in the production of ammonia, well known as a toxic byproduct in mammalian cell cultures [43], yielded the dual benefits of lactate and ammonia reduction in culture. Alanine generation was also greatly reduced in KB26.5-BHRF1, an amino acid that often accumulates in mammalian cell cultures [40]. In any case, a metabolic flux balance is required to evaluate and discuss the possible effects of BHRF1 on the general behavior of the engineered line with respect to the parental cell line. Interestingly, the expression of BHRF1 has an effect on metabolism, improving the efficiency of nutrient usage, which is necessary for cell growth (see Tables 1–3) and the reduction of byproducts.

The engineered KB26.5-BHRF1 hybridoma cell line suffered a modification in its metabolism. BHRF1 is an antiapoptotic protein located in the inner mitochondrial membrane [44]. For this reason, BHRF1 may have somehow affected carbon and NADH/NAD+ transport between cytoplasm and mitochondria. Most of the antiapoptotic genes reported in the literature are known to be bind at the mitochondrial membrane, regulating apoptosis through modulation of mitochondrial permeability, but also playing an important role in the metabolic processes of mitochondria [45]. Dorai et al. (2009) [22] reported the effect of two antiapoptotic genes on the metabolism of CHO, showing an important reduction in the final lactate concentration due to lactate consumption in culture. In addition, engineered cells showed a more efficient nutrient consumption profile and produced fewer byproducts, such as ammonia or alanine, as observed in this study.

Lactate generation in mammalian cell cultures is a well-known challenge that has been extensively studied in recent years [46,47]. At present, the most accepted hypothesis

for the production of lactate is based on the regeneration of the reducing power (NADH) in the cytoplasm due to the high glycolytic fluxes [46,48]. In this regard, there are two ways to regenerate NADH into the cytoplasm: (1) lactate generation and (2) malate-aspartate shuttle [48]. It should be noted that the malate-aspartate shuttle facilitates the regeneration of NADH and increases the TCA cycle flux (importing malate), thereby generating energy in the form of ATP. However, the generation of lactate provokes a total loss of both carbon sources and ATP generation. Therefore, the mechanism of lactate generation may lie in the flux limit of the Malate-Aspartate Shuttle, leading cells to generate lactate and display this wasteful metabolism.

In the breakdown of glucose into two pyruvate molecules, two molecules of ATP and two NADH are generated. Since the inner mitochondrial membrane is impermeable to NADH, the malate-aspartate shuttle works as an indirect transport system. It has been reported that the flux through this transport occurs at lower rates than glycolysis [49], and that the increased LDH activity is due to the inability to transport NADH through the shuttle at the same rates at which it is generated. Under conditions of increased cellular energy demand, higher glycolytic fluxes are observed, and consequently, NADH production rates increase proportionally. Such an increase in the need for NAD^+ regeneration is compensated for by higher LDH activity in the cytosol, as not much increase is observed in the malate-aspartate shuttle fluxes [50].

5. Conclusions

The results presented in this work provide evidence for a beneficial effect of antiapoptotic gene BHRF1 in hybridoma in terms of cell growth, productivity and metabolism, characterized by a more efficient use of nutrients, doubling the cell density in the culture under identical conditions and using the same culture media. The specific productivity of the cells increased two fold, yielding a three-fold increase in the final concentration of IgG3.

The study and comparison of the intracellular fluxes by means of a flux balance analysis of the KB26.5 and KB26.5-BHRF1 engineered cell lines highlighted the interactions and effects of the BHRF1 protein on the metabolic pathways. In short, BHRF1 primarily affected glucose uptake rate, reducing glycolysis by 50% and, consequently, reducing the generation of lactate by more than 60%. Interestingly, the total ATP generation in the engineered KB26.5-BHRF1 cell line decreased significantly due to the lower energy requirements for maintenance, probably due to the lower energy requirements for maintaining ion gradients (reduction in the generation of lactate), although this hypothesis should be tested in future metabolic flux analysis experiments.

The use of antiapoptotic genes has been extensively explored in recent years, as manifest in a recent review about the attenuation of apoptosis in the CHO cell line [12]. Many efforts have been made to determine how these genes affect cell apoptosis; however, the impact they have on protein production, and especially on metabolism, has not yet been clarified. To address this, a strategy to obtain isogenic cell lines should be implemented, as this would make it possible to compare different antiapoptotic genes and their effects.

Supplementary Materials: The following are available online at https://www.mdpi.com/article/10.3390/app11146258/s1: A complete list of all included reactions and metabolites used is freely available in the Supplementary Data 1 in xlsx format.

Author Contributions: Conceptualization, J.J.C., I.M.-M., A.C., C.P. and M.L.; methodology, J.J.C., I.M.-M., P.C., J.P., A.C., C.P. and M.L.; software, P.C. and I.M.-M.; validation, P.C. and I.M.-M.; formal analysis, J.J.C. and I.M.-M.; investigation, J.J.C., I.M.-M., P.C., D.C.-T., J.P., A.C., C.P. and M.L.; resources, J.J.C. and I.M.-M.; data curation, I.M.-M. and D.C.-T.; writing—original draft preparation, I.M.-M. and D.C.-T.; writing—review and editing, J.J.C., I.M.-M., D.C.-T., M.L., A.C. and C.P.; visualization, P.C. and I.M.-M.; supervision, I.M.-M. and J.J.C.; project administration, J.J.C.; funding A.C.; quisition, J.J.C. All authors have read and agreed to the published version of the manuscript.

Funding: This research was funded by FI-DGR (Generalitat de Catalunya, Catalonia, Spain), grant number FI-DGR.

Institutional Review Board Statement: Not applicable.

Informed Consent Statement: Not applicable.

Acknowledgments: The Novo Nordisk Foundation (Denmark) with the two NNF Grant numbers: NNF10CC1016517 and NNF14OC0009473.

Conflicts of Interest: The authors declare no conflict of interest.

References

1. Walsh, G. Biopharmaceutical Benchmarks 2018. *Nat. Biotechnol.* **2018**, *36*, 1136–1145. [CrossRef]
2. Grilo, A.L.; Mantalaris, A. The Increasingly Human and Profitable Monoclonal Antibody Market. *Trends Biotechnol.* **2019**, *37*, 9–16. [CrossRef]
3. Estes, S.; Melville, M. Mammalian Cell Line Developments in Speed and Efficiency. In *Mammalian Cell Cultures for Biologics Manufacturing*; Zhou, W., Kantardjieff, A., Eds.; Advances in Biochemical Engineering/Biotechnology; Springer: Berlin/Heidelberg, Germany, 2013; Volume 139, pp. 11–33. ISBN 978-3-642-54049-3.
4. Wurm, F.M. Production of Recombinant Protein Therapeutics in Cultivated Mammalian Cells. *Nat. Biotechnol.* **2004**, *22*, 1393–1398. [CrossRef]
5. Hnasko, R.M.; Stanker, L.H. Hybridoma Technology. In *ELISA*; Hnasko, R., Ed.; Methods in Molecular Biology; Springer: New York, NY, USA, 2015; Volume 1318, pp. 15–28. ISBN 978-1-4939-2741-8.
6. Coco-Martin, J.M. A Review of Therapeutic Protein Expression by Mammalian Cells. *BioProcess Int.* **2008**, *6*, 28.
7. Arden, N.; Betenbaugh, M.J. Life and Death in Mammalian Cell Culture: Strategies for Apoptosis Inhibition. *Trends Biotechnol.* **2004**, *22*, 174–180. [CrossRef]
8. Zhang, X.; Han, L.; Zong, H.; Ding, K.; Yuan, Y.; Bai, J.; Zhou, Y.; Zhang, B.; Zhu, J. Enhanced Production of Anti-PD1 Antibody in CHO Cells through Transient Co-Transfection with Anti-Apoptotic Genes Bcl-XL and Mcl-1. *Bioprocess Biosyst. Eng.* **2018**, *41*, 633–640. [CrossRef]
9. Casablancas, A.; Gámez, X.; Lecina, M.; Solà, C.; Cairó, J.J.; Gòdia, F. Comparison of Control Strategies for Fed-Batch Culture of Hybridoma Cells Based on on-Line Monitoring of Oxygen Uptake Rate, Optical Cell Density and Glucose Concentration. *J. Chem. Technol. Biotechnol.* **2013**, *88*, 1680–1689. [CrossRef]
10. Smolke, C.D. *The Metabolic Pathway Engineering Handbook: Fundamentals*; CRC Press: Boca Raton, FL, USA; Taylor: London, UK; Francis: New York, NY, USA, 2010; ISBN 978-1-4398-0296-0.
11. Henry, M.N.; MacDonald, M.A.; Orellana, C.A.; Gray, P.P.; Gillard, M.; Baker, K.; Nielsen, L.K.; Marcellin, E.; Mahler, S.; Martínez, V.S. Attenuating Apoptosis in Chinese Hamster Ovary Cells for Improved Biopharmaceutical Production. *Biotechnol. Bioeng.* **2020**, *117*, 1187–1203. [CrossRef] [PubMed]
12. Vives, J.; Juanola, S.; Cairo, J.J. Metabolic Engineering of Apoptosis in Cultured Animal Cells: Implications for the Biotechnology Industry. *Metab. Eng.* **2003**, *9*, 124–132. [CrossRef]
13. Fussenegger, M.; Fassnacht, D.; Schwartz, R.; Zanghi, J.A.; Graf, M.; Bailey, J.E.; Pörtner, R. Regulated Overexpression of the Survival Factor Bcl-2 in CHO Cells Increases Viable Cell Density in Batch Culture and Decreases DNA Release in Extended Fixed-Bed Cultivation. *Cytotechnology* **2000**, *32*, 45–61. [CrossRef] [PubMed]
14. Mastrangelo, A.J.; Hardwick, J.M.; Zou, S.; Betenbaugh, M.J. Part II. Overexpression of Bcl-2 Family Members Enhances Survival of Mammalian Cells in Response to Various Culture Insults. *Biotechnol. Bioeng.* **2000**, *67*, 10. [CrossRef]
15. Simpson, N.H.; Milner, A.E.; Al-Rubeai, M. Prevention of Hybridoma Cell Death by Bcl-2 during Suboptimal Culture Conditions. *Biotechnol. Bioeng.* **1997**, *54*, 1–16. [CrossRef]
16. Tey, B.T.; Singh, R.P.; Piredda, L.; Piacentini, M.; Al-Rubeai, M. Influence of Bcl-2 on Cell Death during the Cultivation of a Chinese Hamster Ovary Cell Line Expressing a Chimeric Antibody. *Biotechnol. Bioeng.* **2000**, *68*, 13. [CrossRef]
17. Majors, B.S.; Betenbaugh, M.J.; Pederson, N.E.; Chiang, G.G. Mcl-1 Overexpression Leads to Higher Viabilities and Increased Production of Humanized Monoclonal Antibody in Chinese Hamster Ovary Cells. *Biotechnol. Prog.* **2009**, *25*, 8. [CrossRef] [PubMed]
18. Sauerwald, T.M.; Oyler, G.A.; Betenbaugh, M.J. Study of Caspase Inhibitors for Limiting Death in Mammalian Cell Culture. *Biotechnol. Bioeng.* **2003**, *81*, 12. [CrossRef]
19. Vives, J.; Juanola, S.; Cairó, J.J.; Prats, E.; Cornudella, L.; Gòdia, F. Protective Effect of Viral Homologues of Bcl-2 on Hybridoma Cells under Apoptosis-Inducing Conditions. *Biotechnol. Prog.* **2003**, *19*, 84–89. [CrossRef]
20. Juanola, S.; Vives, J.; Milián, E.; Prats, E.; Cairó, J.J.; Gòdia, F. Expression of BHRF1 Improves Survival of Murine Hybridoma Cultures in Batch and Continuous Modes. *Appl. Microbiol. Biotechnol.* **2009**. [CrossRef]
21. Xiong, K.; Marquart, K.F.; la Cour Karottki, K.J.; Li, S.; Shamie, I.; Lee, J.S.; Gerling, S.; Yeo, N.C.; Chavez, A.; Lee, G.M.; et al. Reduced Apoptosis in Chinese Hamster Ovary Cells via Optimized CRISPR Interference. *Biotechnol. Bioeng.* **2019**, *116*, 1813–1819. [CrossRef] [PubMed]
22. Dorai, H.; Kyung, Y.S.; Ellis, D.; Kinney, C.; Lin, C.; Jan, D.; Moore, G.; Betenbaugh, M.J. Expression of Anti-Apoptosis Genes Alters Lactate Metabolism of Chinese Hamster Ovary Cells in Culture. *Biotechnol. Bioeng.* **2009**, *103*, 592–608. [CrossRef]
23. Templeton, N.; Lewis, A.; Dorai, H.; Qian, E.A.; Campbell, M.P.; Smith, K.D.; Lang, S.E.; Betenbaugh, M.J.; Young, J.D. The Impact of Anti-Apoptotic Gene Bcl-2Δ Expression on CHO Central Metabolism. *Metab. Eng.* **2014**, *25*, 92–102. [CrossRef] [PubMed]

24. Martínez-Monge, I.; Albiol, J.; Lecina, M.; Liste-Calleja, L.; Miret, J.; Solà, C.; Cairó, J.J. Metabolic Flux Balance Analysis during Lactate and Glucose Concomitant Consumption in HEK293 Cell Cultures. *Biotechnol. Bioeng.* **2018**. [CrossRef] [PubMed]
25. Altamirano, C.; Illanes, A.; Becerra, S.; Cairó, J.J.; Gòdia, F. Considerations on the Lactate Consumption by CHO Cells in the Presence of Galactose. *J. Biotechnol.* **2006**, *125*, 547–556. [CrossRef] [PubMed]
26. Zhang, L.; Shen, H.; Zhang, Y. Fed-Batch Culture of Hybridoma Cells in Serum-Free Medium Using an Optimized Feeding Strategy. *J. Chem. Technol. Biotechnol.* **2004**, *79*, 171–181. [CrossRef]
27. Henry, O.; Durocher, Y. Enhanced Glycoprotein Production in HEK-293 Cells Expressing Pyruvate Carboxylase. *Metab. Eng.* **2011**, *13*, 499–507. [CrossRef] [PubMed]
28. Chen, K.; Liu, Q.; Xie, L.; Sharp, P.A.; Wang, D.I.C. Engineering of a Mammalian Cell Line for Reduction of Lactate Formation and High Monoclonal Antibody Production. *Biotechnol. Bioeng.* **2001**, *72*, 55–61. [CrossRef]
29. Yoon, S.; Konstantinov, K.B. Continuous, Real-Time Monitoring of the Oxygen Uptake Rate (OUR) in Animal Cell Bioreactors. *Biotechnol. Bioeng.* **1994**, *44*, 983–990. [CrossRef]
30. Zhou, W.; Hu, W.-S. On-Line Characterization of a Hybridoma Cell Culture Process. *Biotechnol. Bioeng.* **1994**, *44*, 170–177. [CrossRef]
31. Fontova, A.; Lecina, M.; López-Repullo, J.; Martínez-Monge, I.; Comas, P.; Bragós, R.; Cairó, J.J. A Simplified Implementation of the Stationary Liquid Mass Balance Method for On-Line OUR Monitoring in Animal Cell Cultures. *J. Chem. Technol. Biotechnol.* **2018**, *93*. [CrossRef]
32. Martínez-Monge, I.; Comas, P.; Triquell, J.; Lecina, M.; Casablancas, A.; Cairó, J.J.J. A New Strategy for Fed-Batch Process Control of HEK293 Cell Cultures Based on Alkali Buffer Addition Monitoring: Comparison with O.U.R. Dynamic Method. *Appl. Microbiol. Biotechnol.* **2018**. [CrossRef]
33. Martínez-Monge, I.; Comas, P.; Triquell, J.; Casablancas, A.; Lecina, M.; Paredes, C.J.; Cairó, J.J. Concomitant Consumption of Glucose and Lactate: A Novel Batch Production Process for CHO Cells. *Biochem. Eng. J.* **2019**, *151*, 107358. [CrossRef]
34. Martínez, V.S.; Dietmair, S.; Quek, L.-E.; Hodson, M.P.; Gray, P.; Nielsen, L.K. Flux Balance Analysis of CHO Cells before and after a Metabolic Switch from Lactate Production to Consumption. *Biotechnol. Bioeng.* **2013**, *110*, 660–666. [CrossRef]
35. Quek, L.-E.; Nielsen, L.K. On the Reconstruction of the Mus Musculus Genome-Scale Metabolic Network Model. In Proceedings of the Genome Informatics 2008, Queensland, Australia, 1–3 December 2008; Genome Informatics Series Volume 21. Imperial College Press: London, UK, 2008; pp. 89–100.
36. Sheikh, K.; Förster, J.; Nielsen, L.K. Modeling Hybridoma Cell Metabolism Using a Generic Genome-Scale Metabolic Model of Mus Musculus. *Biotechnol. Prog.* **2005**, *21*, 112–121. [CrossRef]
37. Rocha, I.; Maia, P.; Evangelista, P.; Vilaça, P.; Soares, S.; Pinto, J.P.; Nielsen, J.; Patil, K.R.; Ferreira, E.C.; Rocha, M. OptFlux: An Open-Source Software Platform for in Silico Metabolic Engineering. *BMC Syst. Biol.* **2010**, *4*, 45. [CrossRef] [PubMed]
38. Lewis, N.E.; Hixson, K.K.; Conrad, T.M.; Lerman, J.A.; Charusanti, P.; Polpitiya, A.D.; Adkins, J.N.; Schramm, G.; Purvine, S.O.; Lopez-Ferrer, D.; et al. Omic Data from Evolved E. Coli Are Consistent with Computed Optimal Growth from Genome-Scale Models. *Mol. Syst. Biol.* **2010**, *6*, 390. [CrossRef] [PubMed]
39. Droste, P.; Miebach, S.; Niedenführ, S.; Wiechert, W.; Nöh, K. Visualizing Multi-Omics Data in Metabolic Networks with the Software Omix—A Case Study. *Biosystems* **2011**, *105*, 154–161. [CrossRef] [PubMed]
40. Quek, L.-E.; Dietmair, S.; Krömer, J.O.; Nielsen, L.K. Metabolic Flux Analysis in Mammalian Cell Culture. *Metab. Eng.* **2010**, *12*, 161–171. [CrossRef] [PubMed]
41. McKeehan, W.L. Glutaminolysis in Animal Cells. In *Carbohydrate Metabolism in Cultured Cells*; Springer: New York, NY, USA, 1986; ISBN 978-1-4684-7679-8.
42. Mulukutla, B.C.; Gramer, M.; Hu, W.-S. On Metabolic Shift to Lactate Consumption in Fed-Batch Culture of Mammalian Cells. *Metab. Eng.* **2012**, *14*, 138–149. [CrossRef]
43. Yang, M.; Butler, M. Effects of Ammonia on CHO Cell Growth, Erythropoietin Production, and Glycosylation. *Biotechnol. Bioeng.* **2000**, *68*, 370–380. [CrossRef]
44. Milián, E.; Prats, E.; Cairó, J.J.; Gòdia, F.; Vives, J. BHRF1 Exerts an Antiapoptotic Effect and Cell Cycle Arrest via Bcl-2 in Murine Hybridomas. *J. Biotechnol.* **2015**, *209*, 58–67. [CrossRef]
45. Majors, B.S.; Betenbaugh, M.J.; Chiang, G.G. Links between Metabolism and Apoptosis in Mammalian Cells: Applications for Anti-Apoptosis Engineering. *Metab. Eng.* **2007**, *9*, 317–326. [CrossRef] [PubMed]
46. Hartley, F.; Walker, T.; Chung, V.; Morten, K. Mechanisms Driving the Lactate Switch in Chinese Hamster Ovary Cells. *Biotechnol. Bioeng.* **2018**, *115*, 1890–1903. [CrossRef] [PubMed]
47. Zagari, F.; Jordan, M.; Stettler, M.; Broly, H.; Wurm, F.M. Lactate Metabolism Shift in CHO Cell Culture: The Role of Mitochondrial Oxidative Activity. *New Biotechnol.* **2013**, *30*, 238–245. [CrossRef] [PubMed]
48. Zheng, J. Energy Metabolism of Cancer: Glycolysis versus Oxidative Phosphorylation (Review). *Oncol. Lett.* **2012**, *4*, 1151–1157. [CrossRef] [PubMed]
49. Schantz, P.G.; Sjöberg, B.; Svedenhag, J. Malate-Aspartate and Alpha-Glycerophosphate Shuttle Enzyme Levels in Human Skeletal Muscle: Methodological Considerations and Effect of Endurance Training. *Acta Physiol. Scand.* **1986**, *128*, 397–407. [CrossRef]
50. Robergs, R.A.; Ghiasvand, F.; Parker, D. Biochemistry of Exercise-Induced Metabolic Acidosis. *Am. J. Physiol. Regul. Integr. Comp. Physiol.* **2004**, *287*, R502–R516. [CrossRef]